

Membrane-distillation desalination: status and potential

A.M. Alklaibi, Noam Lior*

*Department of Mechanical Engineering and Applied Mechanics, University of Pennsylvania,
Philadelphia, PA 19104-6315, USA
Tel. +1 (215) 898 4803; Fax +1 (215) 573 6334; email: lior@seas.upenn.edu*

Received 7 November 2003; accepted 19 March 2004

Abstract

This paper presents an assessment of membrane distillation (MD) based on the available state of the art and on our preliminary analysis. The process has many desirable properties such as low energy consumption, ability to use low temperature heat, compactness, and perceivably more immunity to fouling than other membrane processes. Within the tested range, the operating parameters of conventional MD configurations have the following effects: (1) the permeate fluxes can significantly be improved by increasing the hot feed temperature (increasing the temperature from 50 to 70°C increases the flux by more than three-fold), and by reducing the vapor/air gap (reducing the vapor air gap thickness from 5 to 1 mm increase the flux 2.3-fold); (2) the mass flow rate of the feed solution has a smaller effect: increasing it three-fold increases the flux by about 1.3-fold; (3) the concentration of the solute has slight effect: increasing the concentration by more than five-fold decreases the flux by just 1.15-fold; (4) the cold side conditions have a lower effect (about half) on the flux than the hot side; (5) the coolant mass flow rate has a negligible effect; (6) the coolant temperature has a lower effect than the mass flow rate of the hot solution. Fouling effects, membranes used, energy consumption, system applications and configurations, and very approximate cost estimates are presented. The permeate fluxes obtained by the different researchers seem to disagree by an order of magnitude, and better experimental work is needed.

Keywords: Membrane distillation; Desalination; Membranes; Hygrophobic membranes

1. Introduction and objectives

This paper is a status review of membrane distillation (MD) as it is understood from the published literature and from our preliminary analy-

sis [1]. The review covers the concept, the membranes used, the configurations and applications, fouling, energy consumption, and cost estimates. A summary of the main performance parameters and their sensitivity to operating and configuration variables of membrane types used and of aspects recommended for further study is given.

*Corresponding author.

This process was introduced in the late 1960s [2–4], but did not attain commercial status as a water desalination process, partly because membranes with the characteristics most suitable for the process were not available then, especially at reasonable prices. These characteristics include a negligible permeability to the liquids and non-volatile components, high porosity for the vapor phase, a high resistance to heat flow by conduction, a sufficient but not excessive thickness, low moisture adsorptivity [3], and a commercially long life with saline solutions under the operating conditions. Furthermore, the halt in development was partially caused by some negative opinions about the economics of the process (cf. [5]), which were, however, performed long ago and on a far-from-optimal membrane and system. For instance, using typical data, the temperature polarization coefficient for their system was roughly estimated by Schofield et al. [6] to be 0.32. Hence for this system, when the temperature difference between the centers of the hot and cold channels is 10°C , the actual temperature difference across the membrane is only 3.2°C .

The geometry of the model is schematically shown in Fig. 1. The hot saline solution (h) flows in direct contact with hydrophobic microporous membranes (m), and the cold solution (c) flows on the cold side of the membrane. The temperature difference between the hot and cold faces of the membrane causes the vapor pressure of the concentrated solution to be higher than that of the cold fluid; as a result, water starts to evaporate at the hot side of the membrane, penetrates through the membrane pores, and then is convected to and condensed on the cold fluid (c) or condensed in a film (f) on a cooling plate (p).

MD systems can be classified into four configurations, according to the nature of the cold side of the membrane: (1) direct contact membrane distillation (DCMD), in which the membrane is in direct contact only with liquid phases, saline water on one side and fresh water on the

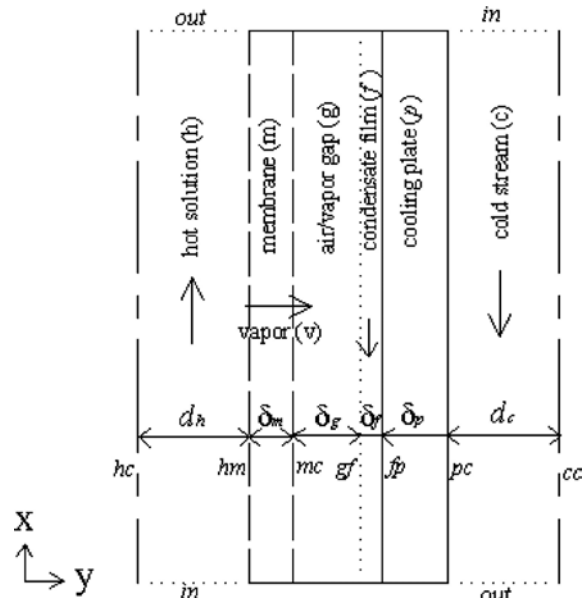


Fig. 1. MD cell configurations; g , f and p included only in AGMD. h : hot solution, m : membrane, g : air gap, f : film condensate, p : cooling plate, c : cold solution for AGMD, cold pure water for DCMD, sweeping air for SGMD, and vacuum for VMD, i : inlet, o : outlet.

other (cf. [7]–[9]); (2) vacuum membrane distillation (VMD), in which the vapor phase is vacuumed from the liquid through the membrane, and condensed, if needed, in a separate device (cf. [10,11]); (3) air gap membrane distillation (AGMD), in which an air gap is interposed between the membrane and the condensation surface (cf. [12,13]); and (4) sweeping gas membrane distillation (SGMD), in which a stripping gas is used as a carrier for the produced vapor, instead of vacuum as in VMD (cf. [14–18]).

Because AGMD and DCMD do not need an external condenser, they are best suited for applications where water is the permeating flux. SGMD and VMD are typically used to remove volatile organic or dissolved gas from an aqueous solution.

2. Membrane materials

2.1. Membrane properties and characteristics

Membranes used in membrane distillation should have the following properties:

1. Be thin, since the permeate flux is inversely proportional to the membrane thickness. The other requirements pertain to the non-wetting condition. The solution brought into contact with the membrane must not penetrate the pores of the membrane. This can be quantified by the Laplace (Cantor) equation

$$\Delta P_{\text{entry}} - \frac{2\gamma_l}{r_{p,\text{max}}} \cos\theta \quad (1)$$

where ΔP_{entry} is the entry pressure difference, γ_l is the surface tension of the solution, θ is the angle of contact between the solution and the membrane surface, and $r_{p,\text{max}}$ is the largest pore size. In view of (1), these non-penetration conditions are:

2. Have reasonably small pore size (r_p , on the order of μm in MD).

3. High surface tension, γ_l , of the feed solution in contact with the membrane.

4. Low surface energy of the membrane material. Membrane materials suitable for MD, which have been used by many researchers, are polytetrafluoroethylene (PTFE), polyvinylidene-fluoride (PVDF), polyethylene (PE), and polypropylene (PP). Those material are hydrophobic (i.e., they have low surface energy). The surface energy of these materials is listed in Table 1.

5. Fouling of the membranes may be an important issue that needs to be investigated further.

Table 2 lists a number of membranes used for MD and their properties with the literature references of the studies in which they were used. The porosity of the membranes used is in the range of 0.06 to 0.85, and the pore size is in the range of 0.2 to 1.0 μm . The thickness is in the range of 0.06 to 0.25 mm with the exception of [22]. The thermal conductivities of polymers are dependent

Table 1

Surface energy of some material used in MD [19]

Membrane material	Surface energy (kJ/m)
PTFE	9.1
PP	30.0
PVDF	30.3
PE	33.2

upon both temperature and the degree of crystallinity [20]. As a result, the reported values of k_m can span a fairly large range: PP, 0.15–0.20 $\text{W m}^{-1}\text{K}^{-1}$; PVDF and PTFE, 0.22–0.45 $\text{W m}^{-1}\text{K}^{-1}$ [21].

2.2. Membrane modules

Different module configurations were used to conduct experimental work in MD. Those used by Kimura and Nakao [30], Banat [13], and Hsu et al. [29] look like the one depicted in Fig. 2a. In this module, a membrane was inserted between two cylindrical compartments (perpendicular to the cylinder axis), with the hot feed solution flowing in one compartments and cold water in the other. The dimensions of these compartments are different for each experimental study. The cylinder has a length of 12 cm and a diameter of 6 cm [29], 15 cm and 8 cm [30], and 15 cm and 5 cm [13]. Separating the two compartments are the membrane, an air gap and a cooling plate in AGMD, and only the membrane in the DCMD configuration.

The modules used by Ohta et al. [39,40] and Liu et al. [36] with an air gap resemble that depicted in Fig. 2b. The dimension of the flow channel [39] is 840 mm long, 390 mm wide, and 80 mm high; 840 mm long, 390 mm wide, and 57 mm high [40]; and 200 mm long, 100 mm wide, and 10 mm high [36].

To avoid the use of membrane supports, the Lawson and Lloyd module [34,35] has a very small square cross sectional area (0.63×0.63 cm),

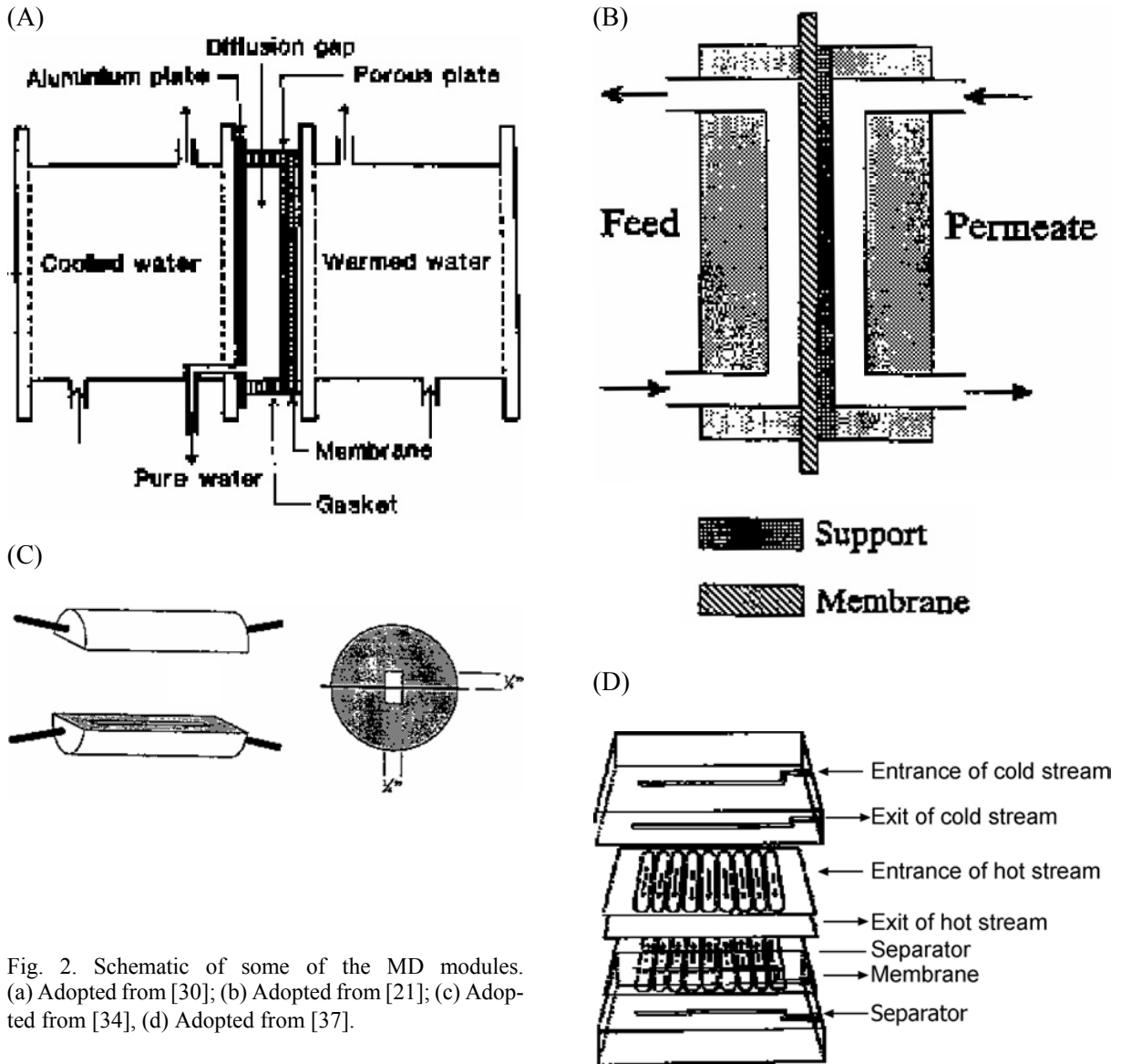


Fig. 2. Schematic of some of the MD modules. (a) Adopted from [30]; (b) Adopted from [21]; (c) Adopted from [34], (d) Adopted from [37].

the same as the channel height, as shown in Fig. 2c.

The modules of Martinez et al. [37] and Martinez and Florido-Diaz [8] look like that depicted in Fig. 2d. This module is composed of two symmetrical rectangular channels between which the flat-sheet membrane is sandwiched. Each compartment is made of nine channels. The dimensions of the channel are 55 mm long, 7 mm wide and 0.4 mm deep.

Some comments on these modules are in order. Because the inlet of the channel in Fig. 2a is off the membrane surface, the evaporation takes place at a temperature and velocity that are lower than that of the inlet, resulting in a lower permeate flux. The modules of Fig. 2b and 2c do not have this shortcoming. However, the channel width for the studies in Fig 2c and Fig. 2d makes

the area of the channel unrepresentative of practical use. The modules do not represent a cell of an integrated MD system.

3. Applications of membrane distillation

AGMD and DCMD are best suited for applications where water is the major permeate component. Several researchers applied these two configurations to produce fresh water from a salt solution. Characteristics of the membranes are listed in Table 2. Table 3 lists the permeate flux they found at the given conditions. Results were in the range between 2.8 and 129 kg/m²h for DCMD and between 5 to 28 kg/m²h for AGMD. The permeate flux average value for all the experiments reported in Table 3 is 26 kg/m²h. The experiments of Ohta et al. [39], Kurokawa and Sawa [32] and Drioli et al. [25] have produced relatively low fluxes compared to that of Lawson and Lloyd [33]. Lawson et al. [33] attributed the higher values to design of the module. Using AGMD, Liu et al. [36] and Banat [13] found almost the same values. But Hsu et al. [29] found 5-fold lower values, maybe because a lower feed temperature was used. Hsu et al. [29] found that the flux produced by DCMD is higher than that produced by AGMD by 8-fold at the same conditions. It should be emphasized that the wide variation of permeate flux among researchers cannot be explained merely by the fact that they used different conditions. It is imperative to know the maximum permeate flux of MD under optimal conditions so that the viability of the process can be assessed and compared with other desalination processes such as RO or MSF. More experimental work needs to be dedicated towards that objective.

For comparison, the range of permeate fluxes in typical commercial RO processes is 12–15 kg/m²h for seawater and 18–26 kg/m²h for brackish water. Since MD fluxes are not very sensitive to salinity, this is up to 9-fold lower than the highest

obtained in the reported MD experiments. In advanced commercial MSF plants they are about 1,200 kg/m²h, about 10-fold higher.

The last column of Table 3 lists the mass transfer coefficient defined as

$$K_M = \frac{Jh_{fg}}{(T_{hi} - T_{ci})} \quad (2)$$

that reaches a value of 1,560 Jm⁻²s⁻¹K⁻¹ in the reported experiments. For comparison, data from an advanced operating MSF plant show that $K_M \sim 11,700 \text{ kg m}^{-2} \text{ s}^{-1}$, 7.5-fold higher. It is important to note though that the dimensions of the MSF plant are orders of magnitude larger than those of a comparable MD plant, and the used material is much heavier and more expensive, discussed in greater detail below.

In addition to producing water, membrane distillation has been used for concentration of juice and wastewater treatment as shown in Table 4. Nene et al. [38] employed MD to concentrate raw cane sugar and found that at steady state; the water flux from the cane sugar was 10 kg/m²h.

4. Effects of the fundamental operating parameters

The fundamental operating parameters of the MD process are the hot feed solution temperature, T_{hi} ; the mass flow rate of feed solution, \dot{m}_h ; the air/vapor gap thickness, δ_g ; and the coolant mass flow rate, \dot{m}_c ; or the circulating sweeping velocity, u_{ci} in the SGMD. This section includes the effects of these parameters on the permeate flux in MD systems.

4.1. Effect of the saline solution temperature

Several researchers have studied the effect of the feed temperature on the permeate flux, and

Table 2
Membranes used by some researchers reviewed in this paper

Reference	Membrane material	ϵ	$r_p, \mu\text{m}$	δ_m, mm	Company	Model
Banat [13]	PVDF	0.75	0.45	0.11	Millipore	N/A
Bandini and Sarti [22]	PP	N/A	0.2	1.5	Akzo-Nobel	Accurel
Basini et al. [14]	pp	N/A	N/A	N/A	N/A	N/A
Calabro et al. [23]	PP	0.70	0.45	N/A	N/A	N/A
Calabro et al. [24]	PVDF	0.75	0.11	0.14	Millipore	N/A
Drioli and Wu [25]	Teflon	N/A	N/A	N/A	Gelman	N/A
	Teflon	N/A	N/A	N/A	Sumitomo Chem.	N/A
Drioli and Wu [26]	PP	0.7	0.43	0.15	Enka AG	N/A
Guijt et al. [27]	N/A	0.5	0.45	0.096	N/A	N/A
Guijt et al. [28]	PP	N/A	0.4–0.6	0.15	Akzo Nobel	PP1 LX150/330
	PP	0.7	0.1	0.055	Mitsubishi	EHF270FA16
	PP	N/A	0.2	0.25	Millipore	UPE
Hanbury and Hodgkiess [5]	PTFE	N/A	N/A	N/A	Goretex	N/A
Hsu et al. [29]	PTFE	0.70	0.20	0.175	Millipore	Fluropore
	PTFE	0.85	0.5	0.175	Millipore	Fluropore
Khayet et al. [15, 16]	PTFE	0.80	0.20	0.178	Gelman Science	TF-200
Khayet et al. [15,16]	PTFE	0.80	0.45	0.178	Gelman Science	TF-450
Kimura and Nakao [30]	PTFE	N/A	0.2–3	0.08	Nitto Electric	N/A
Kubota et al. [31]	PTFE	0.75	N/A	0.1	N/A	N/A
Kurokawa and Sawa [32]	PTFE	N/A	0.20	N/A	N/A	N/A
Lagana et al. [33]	PP	0.7	0.45	0.12	Enka	MD-020-2N-CP
Lawson and Lloyd [34,35]	PP	0.66	0.29	0.091	3M	MA
	PP	0.76	0.40	0.081	3M	MB
	PP	0.79	0.51	0.076	3M	MC
	PP	0.80	0.58	0.086	3M	MD
	PP	0.85	0.73	0.079	3M	ME
Liu et al. [36]	PTFE	0.85	1.0	0.150	Millipore	N/A
Martinez et al. [37]	PTFE	0.80	0.20	0.06	Gelman Instr.	TF200
Martinez and Florido [8]	PVDF	0.70	0.45	0.125	Millipore	Durapore HVHP45
	PVDF	0.75	0.22	N/A	Millipore	Durapore GVHP22
Nene et al. [38]	PP	N/A	0.2	N/A	Akzo	Wuppertal
Ohta et al. [39]	Fluoro-carbon	N/A	N/A	0.13	N/A	N/A
Sarti et al. [41]	PTFE	0.6	1.0	0.6	Gelman Inst.	TF1000
	PTFE	0.6	2.0	0.6	Gelman Inst.	TF200
Schofield et al. [6]	PP	0.75	0.10	0.100	Enka	N/A
	PP	0.75	0.2	0.14	Enka	N/A
	PVDF	0.75	0.45	0.11	Millipore	Durapore
Schofield et al. [42,43]	PVDF	0.75	0.45	0.110	Millipore	Durapore
Ugrozov et al. [44]	Copolymer of PTFE and PVDF	0.7	0.25	0.12	N/A	MFF-2

Table 3
Permeate fluxes and mass transfer coefficients in MD of NaCl solutions, as obtained in several studies

Reference	MD configuration	T_{hi} , °C	T_{ci} , °C	$(T_{hi}-T_{ci})$, °C	w_{si}	δ_{g^2} , mm	Flow rate, l/min	J , kg/m ² h	K_M , J/m ² sK
Hsu et al. [29]	DCMD	45	20	25	0.030	0	3.3	40	1070
Drioli et al. [25]	DCMD	50	20	30	0.0058	0	N/A	5	111
Martinez and Florido [8]	DCMD	50	14	36	0.058	0	1.2	28	519
Kurokawa and Sawa [32]	DCMD	90	50	40	N/A	0	0.31	4.6	77
Lawson and Lloyd [35]	DCMD	75	20	55	0.035	0	3.78	129	1560
Ugrozov et al. [44]	DCMD	70	10	60	0	0	4.17	17	189
Ohta et al. [39]	DCMD	60	25	35	0	0	0.06 m/s	2.8	53
Banat [13]	AGMD	90	7	82	0.001	8	4.5	26	211
Hsu et al. [29]	AGMD	45	20	25	0.03	5	3.3	5	133
Liu et al. [36]	AGMD	75	20	55	0.003	4	3.8	28	339
Guijit et al. [27]	AGMD	90	65	25	0	4	0.02	7	187
Khayet et al. [15]	SGMD	50	20	30	0	N/A	0.21 m/s	21	467

Table 4
Permeate fluxes, as obtained by several studies, in concentration and treatment processes of various liquids (Brix is a scale used to measure dissolved solid concentrations in water)

Reference	Application	Configuration	Feed solution	\dot{m}_h , l/min	w_s	T_{hi} , °C	T_{ci} , °C	p , kPa	$(T_{hi}-T_{ci})$, °C	J , kg/m ² h
Calabro et al. [23]	Wastewater treatment	DCMD	Blue E-G	0.026	0.05	50	45	—	5	0.18
							40		10	0.342
							35		15	0.432
Nene et al. [28]	Concentration of raw cane sugar	DCMD	Sugar cane	1	20 Brix	75	25	—	50	10
							—		—	—
Calabro et al., [24]	Concentration of orange juice	DCMD	Orange juice	5	108 g/l	45	20	—	25	10
						35	15		5.4	
Bandini et al. [22]	Concentration of must	VMD	Glucose	2.5	50 Brix	50	—	0.1	—	5.4
						35	0.1		2.52	
						30 Brix	0.1		7.2	
						35	0.1		2.88	
Lagana et al. [33]	Concentration of apple juice	DCMD	Apple juice	3.3	0.265	32	22	—	10	1
						7	—		25	2

Table 5
Effect of feed temperature on the permeate flux

Reference	Flow rate, l/min	w_s	T_{ci} , °C	Range of T_{hi} , °C	Range of $(T_{hi} - T_{ci})$, °C	n -fold increase in J for given temp. range
Liu et. al. [36]	0.063	0.005	20	50–70	30–50	2.83
Martinez and Florido [8]	0.48	0.058	14	50–70	36–56	3.0
Banat [13]	4.5	0.014	20	50–70	30–50	3.0
Ohta et al.[39]	0.3 m/s	0	25	40–60	15–35	3.5
Jonsson [7]	N/G	0	20	50–70	30–50	3.5
Ugrozov et al. [44]	0.33	0	10	40–70	30–60	3.5

Table 6
Effect of coolant temperature on the permeate flux

Reference	Flow rate, l/min	w_s	T_{hi} , °C	Range of T_{ci} , °C	Range of $(T_{hi} - T_{ci})$, °C	n -fold increase in J for given temp. range
Banat [13]	4.5	0.0125	60	10–30	50–30	1.18
Lawson and Lloyd [33]	3.78	0	59	9–29	50–30	1.4
Jonsson [7]	N/A	0	60	10–30	50–30	2.0
Kurokawa and Sawa [32]	0.31	0	90	25–50	65–40	1.23

Table 5 lists their results. As seen, the feed solution temperature has a major effect on the permeate flux. This increase is larger at higher temperatures because the vapor pressure increases exponentially with temperature.

4.2. Effect of the coolant temperature

The effect of the coolant temperature in several studies is listed in Table 6. The coolant temperature has a more than 2-fold smaller effect on the flux than that of the feed solution for the same temperature difference. This is because the vapor pressure increases more than linearly with temperature.

4.3. Effect of mass flow rate of the feed solution

The effect of the mass flow rate of the feed solution in the hot channel, as found by several researchers, is shown in Table 7. The results

show that the permeate flux increases with the mass flow rate. The effect of the mass flow rate is, however, 2.5-fold weaker than that of the feed temperature. Kubota et al. [30] conducted experiments on membrane distillation and stated that the permeate flux increases with the mass flow rate until it reaches a maximum, and then decreases. Most of the researchers, however, show that the flux increases to an asymptotic value with the increase in mass flow rate (cf. Banat [13]). The boundary layer thickness decreases with the increase in the flow velocity, but then this effect does not change with further increase of the velocity.

4.4. Effect of coolant mass flow rate

The effect of the coolant mass flow rate, as found by different researchers, is shown in Table 8. Banat [7] found that the cooling water flow rate had a minimal effect (not noticeable) on

Table 7
Effect of the feed solution flow rate on the permeate flux

Reference	T_{hi} , °C	T_{ci} , °C	$(T_{hi}-T_{ci})$, °C	w_s	Range of feed flow rate, l/min	n -fold increase in J for given flow rate
Banat [13]	60	20	53	0.033	2–5	1.2
Martinez et al. [37]	N/G	14	—	0.058	0.6–1.2	0.125
Ohta et al. [39]	60	25	35	N/A	0.02–0.08 m/s	1.83
Ugrozov et al. [44]	60	10	50	0	1.33–4.17	1.37

Table 8
Effect of coolant flow rate on the permeate flux

Reference	Range of \dot{m}_c	T_{hi} , °C	T_{ci} , °C	w_s	n -fold increase in J for given \dot{m}_c
Banat [13]	1–5 l/min	60	20	0.104	No noticeable effect
Ohta et al. [39]	0.02–0.08 m/s	60	20	0	1.5

the permeate flux. Ohta et al. [39] found that increasing the coolant velocity from 0.02 to 0.08 m/s resulted in a 1.5-fold increase of the permeate flux. In the same study he showed that hot feed velocity increased the flux by 2.0-fold. This implies that the effect of the coolant velocity is less significant than that of hot feed.

4.5. Effect of the width of the air/vapor gap

The effect of the air/vapor gap width on the permeate flux is listed in Table 9. The results show that the flux increases as the gap is made smaller. The decrease in the air gap increases the permeate flux by about 2-fold. Jonsson et al. [6] reported that the effect of the air gap becomes even more significant for vapor/air gaps thinner than 1 mm.

4.6. Effects of the sweeping gas conditions in SGMD

Table 10 lists the effect of the sweeping gas

velocity as reported by Basini et al. [12] and Khayet et al. [10,19]. It is concluded that the sweeping gas velocity is a crucial operating parameter in determining the process rate, up to a value in which the rate determining resistance is offered by the porous membrane itself. Interestingly, the permeate flux increased with the entrance humidity of the sweeping air, since dry air consumes some of the produced air for its own humidification. The production also increased as gas temperature was decreased, and was weakly affected by the feedwater velocity.

4.7. Effect of feed concentration

Schofield et al. [41] studied experimentally the effect of the concentration of NaCl and sucrose solutions on permeate flux, and found that the flux reduction caused by 30 wt% sucrose is less than that caused by 25% wt% NaCl under the same conditions of feed velocity and temperature and using the same PVDF membrane. This is mainly due to the higher molecular weight

Table 9
Effect of air gap width on the permeate flux

Reference	δ_m , mm	T_{hi} , °C	T_{ci} , °C	w_s	n -fold increase of J as the gap is made smaller in the range tested
Jonsson et al. [12]	5–1	60	20	0	3.5
Liu et al. [36]	5–1	55	20	0.003	2.0
Guijit et al. [27]	5–1	80	65	N/A	2.3

Table 10
Effect of sweeping gas velocity on the permeate flux

Reference	T_{hi} , °C	T_{ci} , °C	u_{ci} , m/s	n -fold increase of J as sweeping gas velocity increases
Basini et al. [14]	58	30	1–3	2
Khayet et al. [15,16]	65	20	0.5–1.5	2

Table 11
Effect of feed solution (aqueous, NaCl) concentration on the permeate flux

Reference	T_{hi} , °C	T_{ci} , °C	Flow rate, l/min	w_s	Percentage decrease in J for given w_s
Banat [13]	55	7	5.5	0.001–0.01	6
Lawson and Lloyd [33]	80	20	3.78	0–0.0754	7

fraction of the sucrose: for the same weight fraction, the mole fraction for sucrose is smaller, resulting in a lower vapor pressure reduction than that due to NaCl, and the main reason for the flux reduction in the sucrose solution is its increased viscosity. Effects of feed concentration reported by others are listed in Table 11.

4.8. Effect of noncondensable gases

In all practical desalination distillation processes, non-condensable gases evolve alongside with the vapor, including both gases dissolved in the feed water and other gases, primarily carbon dioxide from the thermal decomposition of bicarbonates. In membrane distillation these gases will be absorbed into the membrane pores and may

well tend to reduce vapor flux; they are also likely to reduce the condensation heat transfer coefficient.

Another important consideration is that the presence of air may cause the vapor transport rate to be mass transfer limited (because of the additional mass transfer resistance it presents to vapor diffusion) where improved heat transfer coefficients then have a relatively small effect on the flux, and deaerated liquids typically make the transport rate heat transfer limited where improved heat transfer coefficients increase this rate.

A common way to deal with the problem of noncondensables in desalination distillation is to deaerate the feedwater prior to distillation. In MD, the feed and/or the permeate can be deaera-

ted prior to entering the module, which causes the partial pressure of the air in the membrane to decrease due to equilibrium considerations. This way of deaeration will increase the pressure difference across the liquid/gas interface, thus increasing the tendency for membrane wetting [43]. Another technique for reducing the effect of the air is by lowering the pressure of the feed and/or the permeate. This method lowers the pressure difference across the membrane, hence reducing the tendency for the membrane wetting. Using the second method, Schofield et al. [43] studied experimentally the effect of air on the transport through the membrane and on the resulting permeate flux. Using fresh water as feed, air pressures from 100 kPa to 10 kPa, and Durapore PVDF and Enka polypropylene membranes, at temperatures between 25 and 90°C, and temperature differences between 10 and 55°C, they found that deaeration increased the flux by increasing the permeability of the membrane, and although this also resulted in an increase in temperature polarization, the net effect was found to be an increase of the flux by 40% (when the deaeration was extrapolated to zero air pressure) above that of a non-deaerated feed. They also found that deaeration improved the process heat efficiency defined below by Eq. (3) since the resulting increase in permeate flux increased Q_L while keeping Q_C unchanged. This topic deserves more detailed study.

5. Membrane fouling

Fouling is the deposition process of particles, colloids, emulsions, suspensions and macromolecules on or in the membrane, with subsequent detrimental effects on the process and the membrane. The consequences of fouling include foulant adsorption, pore blocking, and cake formation. Fouling obviously has a very important impact on the effectiveness and the life of the membrane.

Lawson and Lloyd [21] stated that fouling is less of a problem in MD than in other membrane separations. The premise is that the pores are relatively large compared to the “pores” or diffusion pathways in RO or ultrafiltration (UF) (both have pore sizes <2 nm, approximately three orders of magnitude smaller than those of MD membranes), which are not as easily clogged.

Despite the large pore advantage, fouling was observed in several experimental studies. Drioli and Wu [25] have measured the variation of the permeate flux with time over a 6-day period for 0.58 wt% NaCl (electrolyte) solutions, with $T_{hi} = 50^\circ\text{C}$ and $T_{ci} = 20^\circ\text{C}$, using a Gelman TF 450 0.45- μm pore membrane. Initially the flux was 5.83 kg/m²h, decreasing during the first 3 days to a constant value of 1.66 kg/m²h. Gryta [37] examined microbial growth in MD by scanning electron microscopy (SEM). The MILLEX-HV membrane filter (Millipore) with a pore diameter of 0.45 μm was used in the study. Tap water at $T_{hi} = 80^\circ\text{C}$, $T_{ci} = 20^\circ\text{C}$ at a velocity of 0.3 m/s was tested for the following two cases:

1. Untreated tap water as the MD feed: autopsy of the membrane surface exposed to the hot water revealed a few bacteria. several species of diatoms, and inorganic deposits of Fe, Ca, Si, Zn, Al, Cl, and F.
2. Tap water pretreated by nanofiltration and the addition of hydrochloric acid (pH = 5): no microorganisms were found after 1400 h of operation.

They also studied NaCl feed solutions ($T_{hi} = 90^\circ\text{C}$, $C_{s,i} = 300 \text{ g NaCl/dm}^3$) containing organic matter originating from animal intestines containing *S. faecalis* bacteria and *Pseudomonas*, and upon autopsy measured *S. faecalis* bacteria at $6.2 \times 10^4 \text{ cells/cm}^2$ on the feed side of the membrane. They concluded that problems resulting from biofouling were significantly lower than those encountered in other membrane processes. For example, in RO a significantly larger number of bacteria, equal to $2.1 \times 10^8 \text{ cells/cm}^2$, was found on the feed side of the membrane [46]. They

attributed the biofouling limitation to operation at high concentration and temperature, but they did not show the fouling extent as a function of temperature and concentration.

Using three different feed solutions: (1) raw seawater, (2) raw water pretreated by 0.1 μm microfiltration, and (3) 3% NaCl, Hsu et al. [29] studied the effect of the type of feed solution on fouling in a DCMD configuration with a PTFE membrane from Millipore at $T_{hi} = 45^\circ\text{C}$, $T_{ci} = 20^\circ\text{C}$ and a 3.3 l/min flow rate. The test period was 160 h. It was found that:

1. The pretreatment of the raw water increases the permeate flux by about 25%.
2. The permeate flux obtained from the 3% NaCl feed solution was twice as high as that obtained from raw seawater.

It is a general conclusion that pretreatment has an important positive influence on MD.

As noted in Section 4.8, deaeration of the feedwater, another pretreatment process, was shown by the small amount of available data to improve performance.

6. Heat efficiency

The process heat efficiency in MD can be defined as

$$\eta_r = \frac{Q_L}{Q_T} \quad (3)$$

where Q_L is the latent heat needed in the evaporation process, and Q_T is the total heat input, both per unit mass of permeate,

$$Q_T = Q_L + Q_C \quad (4)$$

where Q_C is the heat lost by conduction.

Bandini et al. [47] have shown that thermal efficiency for pure water does not depend on the membrane thickness. They defined the two parameters W_1 and W_2 as

$$W_1 = \frac{1}{\frac{1/h_h + 1/h_c}{Kh_{fg}/\delta_m}}, \quad W_2 = \frac{k_m}{Kh_{fg}} \quad (5)$$

where K is the permeability of the membrane. While W_1 is a ratio of the thermal conductivity of the liquid phases to that of the membrane, W_2 involves only properties of the membrane and the latent heat of the liquid, and is independent of membrane thickness. When W_1 is high (>10), the transmembrane flux is controlled by the membrane properties, so that higher fluxes can be achieved by more permeable or thinner membranes. It is also stated in the result that a minimum membrane thickness needs to be exceeded in order to obtain a positive distillate flux. This is important in the case where the temperature difference between the two membrane sides is very small. The presence of the salt may then reduce the temperature at the hot side of the membrane below that at the cold side of the membrane, reversing the flux direction to be from the cold to the hot side. Practically, this case is of no interest in MD since $(T_{hm} - T_{mc})$ by far exceeds the threshold temperature. For instance, for a 20,000 ppm salt (unspecified) solution at $T_{hi} = 60^\circ\text{C}$, the threshold temperature is only 0.13°C [6].

The conductive heat loss Q_C per kg transmembrane flux J is

$$\frac{Q_C}{J} = \frac{R_m}{K} \frac{(T_{hm} - T_{mc})}{(P_{v_{hm}} - P_{v_{mc}})} \quad (6)$$

The coefficient R_m/K was obtained experimentally by Martinez et al. [37] for the PTFE membrane with characteristics listed in Table 2. The experiment was carried out at flow rate of 0.016 l/min and 1 molar feed concentration. The feed water temperature range was 21 to 48°C , and the cold temperature was maintained at 14°C . Under these conditions R_m/K was found to be

Table 12
Conductive heat loss per kg permeate flux and heat efficiency as a function of feed temperature

Reference	T_{hi} , °C	T_{ci} , °C	$(T_{hi} - T_{ci})$, °C	Q_c/J , kJ/kg	η_t
Kubota et al. [31]	35	25	10	550	0.81
	40		15	490	0.83
	45		20	470	0.84
Martinez et al. [37]	29	14	15	4000	0.38
	41		27	3000	0.44
	48		34	2500	0.49
Jonsson et al. [12]	40	20	20	550	0.81
	60		40	250	0.90
	80		60	100	0.96
Banat [13]	40	20	20	650	0.76
	60		40	350	0.85
	80		60	250	0.92

$(56 \pm 0.05)10^7 \text{ kg m s}^{-4} \text{ K}^{-1}$, and a correlation for Q_c/J as a function of $(dP_v)/(dT)$ was developed:

$$\frac{Q_c}{J} = (0.1 \pm 0.3) + (0.56 \pm 0.05) \left(\frac{dP_v}{dT} \right)^{-1} \quad (7)$$

The values of Q_c/J at $T_{hi} = 31, 27,$ and 21°C were found to be around 2500, 3000 and 4000 kJ/kg, respectively. These values, however, are higher than those reported by others, listed in Table 12, and as a consequence his system has low values of η_t . Q_c/J was found to decrease as the operating temperature of the solution increased, and thus the heat efficiency increases as is shown in the last column of Table 12.

7. Energy requirements and cost

7.1. Energy requirements

The input energy needed to raise the temperature of the feed solution to the designed inlet temperature of the hot channel is

$$Q_{\text{req}} = \dot{m}_h C_{pS} (T_{hi} - T_{sr}) \quad (8)$$

where T_{sr} is the temperature of feed solution at the source.

The minimum input energy to produce 1 kg of distillate water is the heat of evaporation ($\sim 2.4 \text{ MJ/kg}$). A portion or all of this high-energy demand can be covered through the following:

- utilizing low-grade waste energy
- MD with heat recovery
- integrating MD with other desalination processes.

7.1.1. Utilizing low-grade waste energy

Using natural waste energy as the heat source, Carlsson [48] built a $5 \text{ m}^3/\text{d}$ MD system, but dimensions and other details were not given. He stated that the power consumption of this process can be as low as 1.25 KWh/m^3 (4.5 KJ/kg produced fresh water), and that the cost would be reduced in a large-scale plant, but did not relate that to the area of the membrane or even the conditions under which this could be attained. This extremely low energy consumption could only have been obtained if the thermal energy consumption had not been included.

7.1.2. MD with heat recovery

The only energy-sensible way to use MD is by incorporating internal heat recovery, as shown in Fig. 3. The heat transferred to the cooling channel

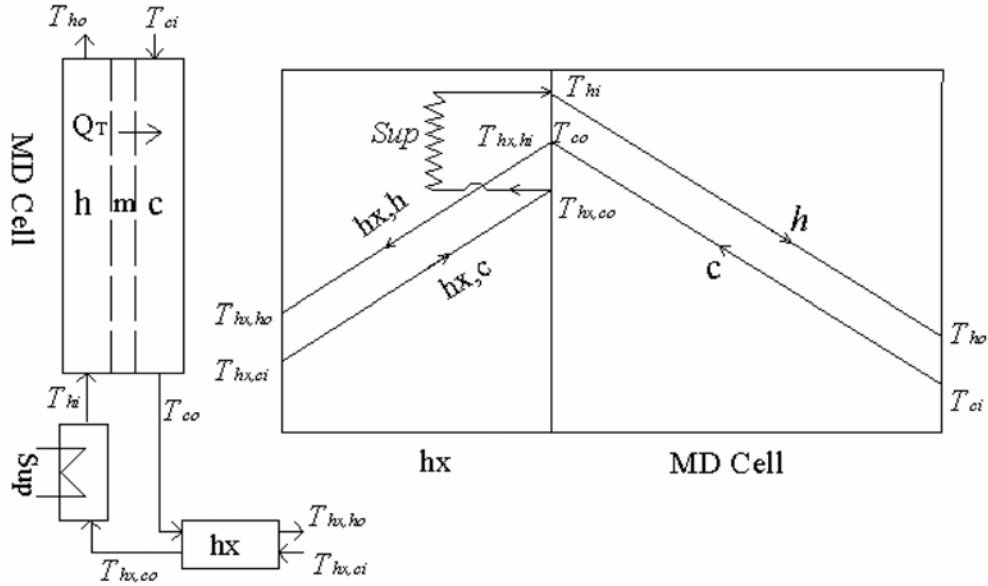


Fig. 3. Membrane distillation cell equipped with heat recovery heat exchanger. h, hot steam; c, cold steam; m, membrane; hx, heat exchanger; Sup, external heat source; hi, inlet of hot channel; ho, outlet of hot channel; ci, inlet of cold channel; co, outlet of cold channel.

by conduction and condensation, Q_T [Eq. (2)], raises the outlet temperature of the water flowing in cooling channel. A portion of Q_T can be recovered to preheat the feed solution so the process heat requirement is reduced. The percentage of the recovery of the heat depends on the heat exchanger effectiveness.

$$\eta_{hx} = \frac{(T_{hx,co} - T_{hx,ci})}{(T_{hx,hi} - T_{hx,ci})} \quad (9)$$

Solving for $T_{ex,co}$, Eq. (9) becomes

$$T_{hx,co} = \eta_{hx}(T_{hx,hi} - T_{hx,ci}) + T_{hx,ci} \quad (10)$$

The input energy from an external source is

$$Q_{req} = \dot{m}_h C_{pS} (T_{hi} - T_{ex,co}) \quad (11)$$

For maximum heat recovery $T_{hx,co}$ should be as high as possible. For high $T_{hx,co}$, η_{hx} should be as close to unity as possible, and $T_{hx,hi}$ should be maximized, but this will decrease $T_{hi} - T_{co}$, and that will lower the permeate flux. Obviously, optimizations should be conducted.

Although many researchers designed their experimental set-up so that heat recovery is utilized, few studied the effect of the heat recovery on the process cost. Schneider et al. [49] mentioned that heat recovery can reduce the cost up to 4-fold. No analysis was shown, neither was the consequent effect on the flux investigated.

A heat recovery heat exchanger was included in the DCMD configuration of Kurokawa and Sawa [32]. For conditions of 90 and 50°C of the hot and cold solutions, respectively, with a flow rate of 0.31 l/min, they showed experimentally that 66% of the latent heat can be recovered, and that 4.6 kg/m²h of permeate flux can be obtained at a heat input of 0.21 kWh.

7.1.3. Integrating membrane distillation with other saline water distillation processes

Using MD as a bottoming process for MSF or ME, so the hot reject brine from MSF or ME is the feed solution for the MD which was not considered yet. Investigation of integrating MD with RO, however, was carried out by Drioli et al. [50]. The reject brine from RO is used as the feed solution for MD. Because MD is much less sensitive to concentration, more fresh water can be produced and the RO brine volume can be furthermore reduced in the MD unit. The reduction of the quantity of brine produced leads to a lower environmental impact. Their cost analysis assuming a MD plant installed at a cost of \$116/m² is summarized in Table 13. It shows that the RO+MD combined plant produced more than twice as much water as the stand-alone RO plant at the same water cost. The stand-alone MD plant produced as much water as the RO+ MD plant, but at a water cost about 5% higher.

7.2. Estimation of the MD cost

The cost of desalination or separation processes varies from location to location as the conditions of the processed water and the nature and the size of the plant are different. Many leading cost components of MD are not yet known because the process has not been applied in commercial size to have the cost benefits of mass production; neither are factors such as permeate flux, pretreatment, fouling and membrane life known adequately yet.

Table 13
Cost and production rate of RO, MD, and RO + MD plants for a fixed membrane area of \$116 m² [39]

Process	Product/feed ratio	Estimated cost of produced water, \$/m ³
Only RO	0.391	1.25
Only MD	0.856	1.32
RO+MD	0.856	1.25

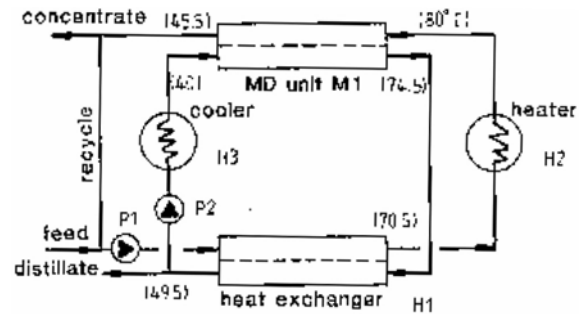


Fig. 4. Flow diagram for MD plant (adopted from Fane et al. [51]).

Table 14
Cost data given by Fane et al. [51]; items in the Unit column correspond to the components in Fig. 4

Unit	Capital, \$	Utility, \$/t
800 m ² hollow fiber MD module	150,000	0
1.4 MW heater (H2)	12,000	2.9
1.4 MW cooler (H3)	12,000	0.2
3.6 MW heat exchangers for heat recovery (H1)	60,000	0
120 m ³ /h, two pumps (P1,P2)	6,000	0.2
	240,000	3.3

Nevertheless, a few cost estimates for some specific cases were made. Fane et al. [51] have estimated the cost for a simple 5000 kg/hr MD plant with heat recovery shown in Fig. 4. The detail costing of the plant is shown in Table 14. For plant capacity (P_{cap}) of 44,000 t/y, the total cost (C_T) was calculated in term of the capital cost (C_{ca}) and operating cost (C_{op}) as

$$C_T = 3 \times C_{ca} \times 0.10/y / (P_{cap}/y) + C_{op} = \$4.9/t \quad (12)$$

They concluded that the costs on this production scale could be similar to those of RO (scaled to 1987).

Table 15
Cost estimation data [11]

Bare module factor (BM)	2
Depreciation (% capital cost), y	15
Labor cost (% of capital cost), y	10
Membrane cost (module), \$/m ³	450
Membrane life, y	3
Hours of operation, y	7200
Pump efficiency	0.8
Electricity, \$/kWh	0.085
Stream at low pressure, \$/kg	0.013
Cooling water	0.15

Sarti et al. [11] roughly estimated the cost of a benzene removal from wastewater containing 1000 ppm of benzene based on the data listed in Table 15, and the capital cost of \$247,000, which was calculated using cost correlations from Woods [52]. They estimated the product cost to be \$4.04/m³.

The process was assessed based on the required area of the membrane per kg permeate flux by Hanbury and Hodgkiess [5] by both experiment and analysis. They derived the following semi-empirical expression to compute the specific membrane area requirement, as

$$\frac{A_m}{J} = \frac{1200.480 C_p}{(T_{h,i} - T_{c,o})} \frac{\dot{m}_h}{J} \left(\frac{1}{T_{c,i}^{0.17}} - \frac{1}{T_{c,o}^{0.17}} \right) \quad (13)$$

where C_p is KJ/kg.k and temperatures are in °C.

For their conditions of $T_{h,i}$ and $T_{c,i}$ of 90°C and 20°C, respectively, and a feed-to-product ratio of 10, the required specific membrane area was found to be 450 m²/(kg/s). The product fluxes in their work were around 27 kg/m²h, near the average obtained by other researchers, shown in Table 3. The prices of some of the membranes that can be used for MD were quoted to us by the Millipore Co. for small quantities and are listed in Table 16. They are quite high, but this also

Table 16
Prices of some membrane materials suitable for MD (Millipore Co. small quantity quotation)

Material type	Price, \$/m ²
PVDF	280
PTFE	753

depends on the life of the membrane and can be reduced significantly in mass production.

8. Some benefits and potential problems of membrane distillation

As discussed in Section 4.7, the MD permeate flux is only slightly affected by the concentration of the feedwater, and thus, unlike other membrane processes, productivity and performance remain roughly the same for high concentration feedwaters. Because the process can be conducted at temperatures typically below 70°C, and driven by low temperature difference (20°C) of the hot and the cold solutions, low-grade waste or solar heat can be used.

The selectivity of membrane desalination is higher than any other membrane process. Pure water produced by MD was quoted to be completely pure when using tap water feeds with concentrations as high as 2450 ppm [49]. As shown in Table 17, the quality was very high compared to the product concentrations of 100 to 500 ppm produced by RO and 50 ppm produced by MSF [53].

MD membranes can be fabricated from chemically resistant polymers. Since the membranes in MD act primarily as a support for a vapor–liquid interface and do not react electrochemically with the solution, they can be fabricated from almost any chemically resistant polymers with hydrophobic intrinsic properties, and that increases membrane life.

MD systems can be very compact. In comparison with conventional MSF process, the

Table 17
Quality of water produced by MD

Reference	Feed conc., ppm	Quality, ppm
Banat [7]	50,000	140
Kubota et. al. [31]	N/G	0.7
Hanbury and Hodgkiess [5]	20,000	1.7
Hsu et al. [18]	30,000	8.4

height of the MSF stage usually in the range of 4–6 m as compared with the height of the ~1 cm height of a MD cell; 1 m² of MD membrane will thus have a volume of 0.01 m³ and produce, with current generation configurations, up to 129 kg/m³h (Table 3), yielding a volumetric production rate of 12,900 kg/m³h. The corresponding production rate per m² of plant surface area for MSF is 306.7 kg/m²h [54], and considering a 4-m stage height, the MSF process has a volumetric production rate of 76.6 kg/m³h, about 40 times lower.

The energy efficiency of optimized MD plants with internal heat recovery can be close to that of commercial MSF plants. A rough estimate is made here for a MD plant producing 1,000 m³/d with heat recovery (Fig. 2) and with no attempt to optimize performance, operating at $T_{hi} = 75^{\circ}\text{C}$, $T_{ci} = T_{hx,co} = 20^{\circ}\text{C}$, $T_{hx,hi} = 70^{\circ}\text{C}$, a modest recovery heat exchanger efficiency of $\eta_{hx} = 0.8$, an experimentally obtained product flux of $J = 129 \text{ kg/m}^2\text{h}$ (0.0358 kg/m²s). The highest flux produced by MD listed in Table 3 to be on the optimistic side for a 3% NaCl solution results in a membrane area requirement of 323 m². The saline solution flow rate was thus calculated to be 122 kg/s, and choosing a flow channel depth of 0.002 m, and the solution velocity corresponding to the J in the cited experiments, $u_h \approx u_c = 1 \text{ m/s}$ ($Re = 5700$), and assuming for simplicity a single hot solution channel and single cold solution heat recovery channel, the channel length is 5.3 m and

width 61 m. The heat demand based on Eq. (10) is estimated then as 660 kJ/kg, equivalent to a performance ratio of 3.6 (this can be improved significantly in an optimized plant). Assuming a pump efficiency of 0.85 but considering only the pumping power needed for flow through the MD channels, the pumping power consumption is 0.96 kJ/kg–0.0003 kWh/kg, more than an order of magnitude lower compared with a typical value of 0.005 kWh/kg in commercial MSF plants [54].

It is likely that in MD with heat recovery the permeate flux will be lower than assumed above because the local driving temperature difference is kept smaller. It is noteworthy that this would not affect the heat consumption, but would proportionally increase membrane area, channel length, and pumping power. Thus, if the flux were reduced 5-fold, the pumping power was found to increase to about 0.0015 kWh/kg, still much lower than that needed for MSF.

Since MD is not used massively in commercial applications, the information about ultimate membrane cost is unavailable to the extent that is in other membrane processes such as RO.

A key technical requirement is that the membranes allow only vapor (and gas) to pass, and not the feed liquid. This is interpreted by the membrane wetting condition [Eq. (1)], and any process conditions that lead to pore flooding will at the least impair product quality, but at most will incapacitate the process. Conditions that may cause such problems include membrane aging, fouling, and feedwater contamination by surfactants, but there have not yet been studies in sufficient detail.

9. Conclusions and recommendations

The operating parameters of conventional MD configurations have the following effects: (1) the permeate fluxes can significantly be improved by increasing the hot feed temperature (increasing the temperature from 50 to 70°C increases the

flux by more than three-fold), and by reducing the vapor/air gap (reducing the vapor air gap thickness from 5 to 1 mm increased the flux 2.3-fold); (2) the mass flow rate of the feed solution has a smaller effect: increasing it three-fold increases the flux by about 1.3-fold; (3) the concentration of the solute has a slight effect: increasing the concentration by more than five-fold decreases the flux by just 1.15-fold; (4) the cold side conditions have a lower effect on the process than the hot side (the ratio of the increase in the permeate flux when hot feed temperature increased to that when the cold temperature decreases by the same quantity is about 2; (5) the coolant mass flow rate (within the tested range) has a negligible effect; (6) the coolant temperature has a lower effect than the mass flow rate of the hot solution.

The heat consumption for MD with heat recovery is comparable to that of MSF plants, but the pumping power is estimated to be much lower.

MD has some significant advantages over other processes, including low sensitivity to feed concentration and the ability to operate at low temperatures and thus uses energy sources such as waste or solar heat, ability to use relatively cheap and robust membranes, higher resistance to fouling than other membrane desalination processes, product quality comparable with other distillation processes and higher than that from RO, and high system compactness. There is potential for significant reduction in costs as a consequence of mass production of membranes and improved internal transport.

The paucity of experimental data and the large scatter in the results indicate that a more intensive and focused research effort in this field is needed, both in experimentation and modeling, where a central issue is the long-term liquid/vapor selectivity of the membranes, followed by the construction of pilot plants for scale-up studies.

10. Symbols

A_m	—	Membrane area, m ²
C_{ca}	—	Capital cost, \$/ton
C_{op}	—	Operating cost, \$/ton
C_p	—	Specific heat, kJ kg ⁻¹ K ⁻¹
C_T	—	Total cost, \$/t
h	—	Heat transfer coefficient, W m ⁻² K ⁻¹
h_{jg}	—	Latent heat of evaporation, kJ kg ⁻¹
J	—	Length-averaged permeate flux at hot side of the membrane, kg m ⁻² h ⁻¹
K	—	Membrane permeability, s ⁻¹
K_M	—	Mass transfer coefficient, J m ⁻² s ⁻¹ K ⁻¹
k	—	Thermal conductivity, W m ⁻¹ K ⁻¹
\dot{m}	—	Mass flow rate, kg s ⁻¹
p	—	Cooling plate
P_v	—	Water vapor pressure, Pa
P_{cap}	—	Plant capacity, ton/y
Q	—	Heat transferred, kJ m ⁻² h ⁻¹
R	—	Thermal resistance, m ² K W ⁻¹
r_p	—	Membrane pore size, m
$r_{p,max}$	—	Largest membrane pore size, m
T_{ci}	—	Inlet temperature of cold solution, °C
T_{hi}	—	Inlet temperature of hot solution, °C
u	—	Feed solution velocity, m/s
w_{si}	—	Mass fraction of salt in solution at the inlet of the channel
W_1, W_2	—	Constants in Eq. (5)
x	—	Coordinate along the solution flow
y	—	Coordinate normal to the solution flow
<i>Greek</i>		
ΔP_{entry}	—	Entry pressure difference, Pa
δ	—	Thickness, m
ε	—	Porosity of the membrane
γ_1	—	Surface tension of liquid, N m ⁻¹
η_{hx}	—	Heat exchanger effectiveness, Eq. (9)

- η_t — Process thermal efficiency, Eq. (3)
 θ — Angle of contact between solution and membrane surface

Subscripts

- C — Sensible heat
 c — Cold solution
 h — Hot solution
 hm — Membrane hot side
 hx — Heat exchanger
 i — Inlet of the channel
 L — Latent heat
 m — Membrane
 mc — Membrane cold side
 o — Outlet of the channel
 T — Total
 v — Vapor

Acknowledgment

The authors are grateful to the Middle East Desalination Research Center for a grant that partially supported this study.

References

- [1] A.M. Klaibi and N. Lior, Transport analysis in membrane distillation, Proc. IDA World Congress on Desalination and Water Reuse, Manama, Bahrain, IDA, Topsfield, MA, USA, 2002.
- [2] P.K. Weyl, Recovery of demineralized water from saline waters. United States Patent 3,340,186, 1967.
- [3] M.E. Findley, Vaporization through porous membranes, Ind. Eng. Chem. Des. Dev., 6 (1967) 226–230.
- [4] M.E. Findley, V.V. Tanna, Y.B. Rao and C.L. Yeh, Mass and heat transfer relations in evaporation through porous membranes, AIChE J., 15 (1969) 483–489.
- [5] W.T. Hanbury and T. Hodgkiess, Membrane distillation — an assessment, Second World Congr. Desalination & Water Re-Use, 3 (1985) 287–297.
- [6] R.W. Schofield, A.G. Fane and C.J.D. Fell, Heat and mass transfer in membrane distillation, J. Membr. Sci., 33 (1987) 299–313.
- [7] K.W. Lawson and D.R. Lloyd, Membrane distillation. II. Direct contact MD, J. Membr. Sci., 120 (1996) 123.
- [8] L. Martinez-Diez and F.J. Florido-Diaz, Theoretical and experimental studies on membrane distillation, Desalination, 139 (2001) 373–379.
- [9] J. Phattaranawik and R. Jiratananon, Direct contact membrane distillation: effect of mass transfer on heat transfer, J. Membr. Sci., 188 (2001) 137.
- [10] S. Bandini, C. Gostoli and G.C. Sarti, Separation efficiency in vacuum membrane distillation, J. Membr. Sci., 73 (1992) 217–229.
- [11] G.C. Sarti, C. Gostoli and S. Bandini, Extraction of organic components from aqueous streams by vacuum membrane distillation, J. Membr. Sci., 80 (1993) 21–33.
- [12] A.S. Jonsson, R. Wimmerstedt and A.C. Harrysson, Membrane distillation — A theoretical study of evaporation through microporous membranes, Desalination, 56 (1985) 237–249.
- [13] F.A. Banat, Membrane distillation for desalination and removal of volatile organic compounds from water, Ph.D. Thesis, McGill University, 1994.
- [14] L. Basini, G. D'Angelo, M. Gobbi, G.C. Sarti and C. Gostoli, A desalination process through sweeping gas membrane distillation, Desalination, 64 (1987) 245–257.
- [15] M. Khayet, P. Godino and J. I. Mengual, Theory and experiments on sweeping gas membrane distillation, J. Membr. Sci., 165 (2000) 261–272.
- [16] M. Khayet, P. Godino and J.I. Mengual, Nature of flow on sweeping gas membrane distillation, J. Membr. Sci., 170 (2000) 243–255.
- [17] C.A. Rivier, M.C. Garcia-Payo, I.W. Marison and U. von Stocker, Separation of binary mixtures by thermostatic sweeping gas membrane distillation I. Theory and simulations, J. Membr. Sci., 201 (2002) 1–16.
- [18] M.C. Garcia-Payo, C.A. Rivier, I.W. Marison and U. von Stocker, Separation of binary mixtures by thermostatic sweeping gas membrane distillation II. Experimental results with aqueous formic acid solutions, J. Membr. Sci., 198 (2002) 197–210.

- [19] M. Mulder, *Basic Principles of Membrane Technology*, 2nd ed., Kluwer, Dordrecht, 1996.
- [20] D.W. van Krevelen, *Properties of Polymers*, 3rd ed., Elsevier, Amsterdam, 1990.
- [21] K.W. Lawson and D.R. Lloyd, Review membrane distillation, *J. Membr. Sci.*, 124 (1997) 1–25.
- [22] S. Bandini and G.C. Sarti, Concentration of must through vacuum membrane distillation, *Desalination*, 149 (2002) 253–259.
- [23] V. Calabro, E. Drioli and F. Matera, Membrane distillation in the textile wastewater treatment, *Desalination*, 83 (1991) 209–224.
- [24] V. Calabro, B.L. Jiao and E. Drioli, Theoretical and experimental study on membrane distillation in the concentration of orange juice, *Ind. Eng. Chem. Res.*, 33 (1994) 1803–1808.
- [25] E. Drioli and Y. Wu, Membrane distillation: an experimental study, *Desalination*, 53 (1985) 339–346.
- [26] E. Drioli, Y. Wu and V. Calabro, Membrane distillation in the treatment of aqueous solution, *Desalination*, 33 (1987) 277–284.
- [27] C.M. Gujjit, I.G. Racz, J.W. van Heuven, T. Reith and A.B. de Haan, Modeling of a transmembrane evaporation module for desalination of seawater, *Desalination*, 126 (1999) 119–125.
- [28] C.M. Gujjit, G.W. Meindersma, T. Reith and A.B. de Haan, Method for experimental determination of the gas transport properties of highly porous fibre membranes: a first step before predictive modeling of a membrane distillation process, *Desalination*, 147 (2002) 127–132.
- [29] S.T. Hsu, K.T. Cheng and J.S. Chiou, Seawater desalination by contact membrane distillation, *Desalination*, 143 (2002) 279–287.
- [30] S. Kimura and S. Nakao, Transport phenomena in membrane distillation, *J. Membr. Sci.*, 33 (1987) 285–298.
- [31] S. Kubota, K. Ohta, I. Hyano, M. Hirai, K. Kikuchi and Y. Murayama, Experiments on seawater distillation by membrane distillation, *Desalination*, 69 (1988) 19–26.
- [32] H. Kurokawa and Toshio Sawa, Heat recovery characteristics of membrane distillation, *Heat Transf. Jap. Res.*, 25 (1996) 3.
- [33] F. Lagana, G. Barbieri, E. Drioli, Direct contact membrane distillation: modeling and concentration experiments, *J. Membr. Sci.*, 166 (2000) 1–11.
- [34] K.W. Lawson and D.R. Lloyd, Membrane distillation. I. Module design and performance evaluation using vacuum membrane distillation, *J. Membr. Sci.*, 120 (1996) 111–121.
- [35] K.W. Lawson and D.R. Lloyd, Membrane distillation. II. Direct contact MD, *J. Membr. Sci.*, 120 (1996) 123–133.
- [36] G.L. Liu, C. Zhu, C.S. Cheung and C.W. Leung, Theoretical and experimental studies on air gap membrane distillation, *Heat Mass Transf.*, 34 (1998) 329–335.
- [37] L. Martinez-Diez, F.J. Florido-Diaz and M.I. Vazquez-Gonzalez, Study of evaporation efficiency in membrane distillation, *Desalination*, 126 (1999) 193–198.
- [38] S. Nene, S. Kaur, K. Sumod, B. Joshi and K.S.M.S. Raghavarao, Membrane distillation for the concentration of raw cane-sugar syrup and membrane clarified sugarcane juice, *Desalination*, 147 (2002) 157–160.
- [39] K. Ohta, K. Kikuchi, I. Hayano, T. Okabe, T. Goto, S. Kimura and H. Ohya, Experiments on seawater desalination by membrane distillation, *Desalination* 78 (1990) 177–185.
- [40] K. Ohta, I. Hayano, T. Okabe, T. Goto, S. Kimura and H. Ohya, Membrane distillation with fluorocarbon membranes, *Desalination*, 81 (1991) 107–115.
- [41] G.C. Sarti, C. Gostoli and S. Matulli, Low energy cost desalination processes using hydrophobic membranes, *Desalination*, 56 (1985) 277–286.
- [42] R.W. Schofield, A.G. Fane, C.J.D. Fell and R. Macoun, Factors affecting flux in membrane distillation, *Desalination*, 77 (1990) 279–294.
- [43] R.W. Schofield, A.G. Fane and C.J.D. Fell, Gas and vapour transport through microporous membranes. II. Membrane distillation, *J. Membr. Sci.*, 53 (1990) 173–185.
- [44] V.V. Ugrozov, I.B. Elkina, V.N. Nikulin and L.I. Kataeva, Theoretical and experimental research of liquid-gas membrane distillation process in membrane module, *Desalination*, 157 (2003) 325–331.
- [45] M. Gryta, The assessment of microorganism growth in the membrane distillation system, *Desalination*, 142 (2002) 79–88.
- [46] H.S. Vrouwenvelder, J.A.M. van Paassen, H.C. Folmer, Jan A.M.H. Hofman, M.M. Nederlof and D. van der Kooij, Biofouling of membranes

- for drinking water production, *Desalination*, 118 (1998) 157–166.
- [47] S. Bandini, C. Gostoli and G.C. Sarti, Role of heat and mass transfer in membrane distillation process, *Desalination*, 81 (1991) 91–106.
- [48] L. Carlsson, The new generation in seawater desalination SU membrane distillation system, *Desalination*, 45 (1983) 221–222.
- [49] K. Schneider, W. Holz and R. Wollbeck, Membranes and modules for transmembrane distillation, *J. Membr. Sci.*, 39 (1988) 25–42.
- [50] E. Drioli, F. Lagana, A. Criscuoli and G. Barbieri, Integrated membrane operations in desalination process, *Desalination*, 122 (1999) 141–145.
- [51] A.G. Fane, R.W. Schofield, and C.J.D. Fell, The efficient use energy in membrane distillation, *Desalination*, 64 (1987) 231–243.
- [52] D.R. Woods, Cost estimation for the process industry, McMaster University, Hamilton, Ont., 1993.
- [53] B. Van der Bruggen and C. Vandecasteele, Distillation vs. membrane filtration: overview of process evolutions in seawater desalination, *Desalination*, 143 (2002) 207–218.
- [54] H.T. EL-Dessouky and H.M. Ettouney, *Fundamentals of Salt Water Desalination*, Elsevier, Amsterdam, 2002.